This is a preprint, the final version is subject to change, of the American Mineralogist (MSA)
Cite as Authors (Year) Title. American Mineralogist, in press.
DOI: https://doi.org/10.2138/am-2019-6860

REVISION 1

Chessboard structures: atom-scale imaging of homologues from the kobellite series

Wei Li[1,2,3], Cristiana L. Ciobanu[1,*], Ashley Slattery[4], Nigel J. Cook[1], Wenyuan Liu[1,5], Benjamin P. Wade[4], Guiqing Xie[2]

[1] *School of Chemical Engineering, The University of Adelaide, Adelaide, SA, 5000, Australia*

[2] *Key Laboratory of Metallogeny and Mineral Assessment, Institute of Mineral Resources, Chinese Academy of Geological Sciences, Beijing 100037, China*

[3] *Faculty of Earth Resources, China University of Geosciences, Wuhan 430074, China*

[4] *Adelaide Microscopy, The University of Adelaide, Adelaide, SA, 5000, Australia*

[5] *College of Zijin Mining, Fuzhou University, 350108 Fuzhou, China*

Abstract: High-angle annular dark field scanning transmission electron microscopy is a powerful Z-contrast technique able to depict the structural motifs in Pb-(Bi-Sb)-sulfosalts. Using two homologues from the kobellite homologous series, a group of "chessboard derivative structures", represented by Bi-, and Sb-rich pairs of natural phases (the kobellite-tintinaite isotypic series and giessenite-izoklakeite homeotypic series), we visualise the slabs underpinning crystal structural modularity for the N=2 homologue kobellite and the N=4 homologue, in this case a Bi-rich izoklakeite (Sb/Sb+Bi=0.35). The homologue number, N, can be readily calculated as $N=n_1/6-1$ and $N=n_2/4$, where n_1 and n_2 are the number of atoms in the PbS- and SnS-motifs, respectively. Atom-scale imaging of thinned foils extracted *in-situ* from samples for which compositional data are available also reveals syntactic unit-cell-scale intergrowths on [001] zone axis with $a_{\text{kobellite}}$ || $b_{\text{izoklakeite}}$. These are as small as half-unit cells of $b_{\text{izoklakeite}}$ and one-unit cell $a_{\text{kobellite}}$. Replacement relationships are also observed as irregular slabs of kobellite 'intruding' into izoklakeite. Both banded and irregular intergrowths account for the compositional fields measured at the μm-scale.

* corresponding author: cristiana.ciobanu@adelaide.edu.au

Keywords: HAADF STEM, chessboard structures, izoklakeite, kobellite.

INTRODUCTION AND BACKGROUND

Direct nanoscale visualisation of the crystal structures of complex minerals by scanning transmission electron microscope (STEM) imaging offers unparalleled insights against which crystal structural models can be validated, and microprobe-scale non-stoichiometry understood in terms of nanoscale heterogeneity. The use of Z-contrast techniques such as high-angle angular dark field (HAADF) STEM imaging is particularly relevant for enhanced high-resolution imaging of structures containing elements with heavier atomic mass (Utsunomiya et al. 2004) and is thus well-suited to many ore minerals (e.g., Xu et al. 2014; Ciobanu et al. 2016; Cook et al. 2017). The complex family of sulfosalts is one such mineral group where HAADF STEM atomic-scale imaging has allowed visualisation of modular Pb-Bi-sulfosalt structures such as cuproneyite (Ciobanu et al. 2016).

Sulfosalts are compounds chemically related to sulfides but containing one or more metalloids (Bi, Sb, As) as cations according to the general formula: $(Me^{+},Me^{2+},etc.)_x[(Bi,Sb,As)^{3+}, Te^{4+}]_y[(S,Se,Te)^{2-}]_z$, where Me^{n+} are various metals (Moëlo et al. 2008). This formula is a simplification as oxy-sulfosalts are also recognised (e.g., Kryukova et al. 2005; Doussier et al. 2008; Biagioni and Moëlo 2017) The ability of metals and metalloids to form various coordination polyhedra, such as $(Bi,Pb,Ag)S_6$ octahedra, bi-caped prismatic PbS_9 polyhedra, or $(Sb,As)S_4$ square-pyramidal coordination, opens-up a broad range of block modularity in which structural motifs formed by the same polyhedral types are combined by symmetry operators, e.g., twin, shear or inversion planes, etc., leading to some of the largest crystal structures and their derivatives (e.g., Makovicky 1997). Smaller metals such as Cu, Fe, and in some cases Ag, occur within interstitial tetrahedral sites. A focus of debate for sulfosalt classification is the disagreement between the crystal-structural restrictions imposed on chemistry/substitution mechanisms and the broad compositional fields identified for many sulfosalts (Moëlo et al. 2008, and references therein). Secondly, these minerals are ideal for the study of non-stoichiometry versus structural disorder

since the presence of micron- to nanoscale intergrowths among species from the same or related series appears to be an inherent characteristic rather than the exception (e.g., Ciobanu and Cook 2000; Ciobanu et al. 2004; Pring et al. 1999; Pring and Ciobanu 2008).

Sulfosalt classification is based upon the structural motifs formed by polyhedral arrangements corresponding to equivalent planes of PbS and SnS structures considered as archetypes for series of Pb-Bi- and Pb-(Bi, Sb)-sulfosalts, respectively (Makovicky 1997). The kobellite homologous series belongs to the wider family of Pb-(Bi, Sb)-sulfosalts and is defined as: $2(Cu,Fe)_2M_{10N+6}S_{11N+13}$ for a 4Å-repeat subunit of the structure, where M=Sb and Bi, and N is the homologue number (Zakrzewski and Makovicky 1986; Makovicky and Mumme 1986; Fig. 1a-c). The series includes two homologues, each represented by Bi-, and Sb-rich pairs of natural phases that currently classified as "chessboard derivative structures" (Moëlo et al. 2008): N=2 for the kobellite-tintinaite isotypic series; and N=4 for the giessenite-izoklakeite homeotypic series.

Giessenite, (monoclinic) was described from the type locality Giessen (Switzerland) by Graeser (1963), with additional data provided by Graeser and Harris (1986) and Makovicky and Karup-Møller (1986). The two specimens have Sb/(Sb+Bi) ratio of 0.195 and 0.146, respectively. The Sb-rich end-member of the series, izoklakeite (orthorhombic), was first defined by Harris et al. (1986) from the type locality (Izok Lake, N.W.T., Canada; Sb/(Sb+Bi) = 0.527). In the same year species of comparable composition (Sb/(Sb+Bi)=0.453-0.555) were described from Vena, Sweden (Makovicky and Mumme 1986; Zakrzewski and Makovicky 1986). Additional compositional and structural data for Bi-richer izoklakeite from other localities [Sb/(Sb+Bi) = 0.391-0.395] was subsequently provided by Armbruster and Hummel (1987) and Ozawa et al. (1998). Members of the giessenite-izoklakeite series commonly co-exist with other Pb-(Bi,Sb)-sulfosalts, notably the kobellite-tintinaite series (Harris et al. 1968; Miehe 1971; Moëlo et al. 1984, 1995).

Despite the common association between the two homologues of the kobellite series, no prior studies

have either addressed their lattice-scale intergrowths, or directly imaged the crystal-structural models considered to underpin homology in the series. In the present study, we use transmission electron microscopy (BF and HAADF STEM) imaging to address such issues in kobellite homologues found in Au-rich ores from the Gutaishan deposit, Southern China (Li et al. 2019a). Results show the modules accounting for homology in chessboard structures are readily identifiable by such methods. Lattice-scale intergrowths reveal both primary banding and replacement relationships.

SAMPLES AND METHODOLOGY

The Guitashan Au deposit is rich in Pb-Cu-Sb-As-sulfosalts (Li et al. 2019b) but also contains stringer zones in which Pb-(Bi,Sb)-sulfosalts and subordinate Bi-tellurides are instead associated with gold. Six thin foils for S/TEM study were prepared using focussed ion beam (FIB)-SEM methods from several areas in a single polished block (Fig. A1, Appendix[1]). Sulfosalts occur as micron-scale intergrowths with one another and also with galena adjacent to coarse native gold and Bi-tellurides (Fig. A1, Appendix[1]). FIB-cuts were placed on areas assessed by electron probe microanalysis (EPMA); compositional data are given in Table A1 Appendix[1]. Each foil was screened by TEM to check sulfosalt orientation on the [001] zone axis to allow imaging of the relevant crystal structural motifs. Of the six foils, one fulfilled such condition and was studied using HAADF STEM imaging. EPMA data was obtained on a Cameca SX-Five Electron Probe Microanalyser (EPMA) running Probe Software (Donovan et al. 2016). Operating conditions and analysis details are given in the Appendix[1].

Thinned foils were extracted in-situ and thinned (to <100 nm) by ion beam (Ga^+) milling using a FEI Helios Nanolab 600 instrument. The TEM foils were attached to Cu grids. Electron diffractions and imaging in BF-mode were performed on a Philips CM200 TEM operated at 200 kV. The instrument is equipped with a LaB_6 source, double tilt holder and Gatan Orius digital camera. Energy-dispersive X-

[1] Deposit item.

ray spectra (EDS) were acquired using an Oxford Instruments X-Max 65T SDD detector running Aztec software. Image and diffraction measurements were performed using DigitalMicrograph™ 3.11.1. HAADF STEM imaging and EDX spot analysis/mapping were performed using an ultra-high resolution, probe corrected, FEI Titan Themis S/TEM operated at 200 kV. This instrument is equipped with an X-FEG Schottky source and Super-X EDS geometry. The Super-X EDS detector provides geometrically symmetric EDS detection with an effective solid angle of 0.8 Sr. Probe correction delivered sub-Ångstrom spatial resolution, and an inner collection angle greater than 50 mrad was used for HAADF experiments using the Fischione HAADF detector. Diffraction indexing was obtained using Winwulff© 1.5.2 software and publicly available data from the American Mineralogist Crystal Structure Database. Visualisations of crystal structure were carried out using CrystalMaker® version 10.1.1 and STEM for xHREM™ version 4.1 software. All instruments are housed at Adelaide Microscopy.

RESULTS AND DISCUSSION

The two sulfosalts in the association are kobellite and Bi-rich izoklakeite (Sb/Sb+Bi=0.35) with empirical formulae: [1] $(Cu_{3.78}Fe_{0.5})_{4.28}(Ag_{0.1}Pb_{20.39}Cd_{0.09}Sb_{12.13}Bi_{19.16})_{51.87}$ $(S_{69.86}Se_{0.07})_{69.93}$; and [2] $(Cu_{3.99}Fe_{0.04})_{4.03}(Ag_{0.55}Pb_{51.32}Cd_{0.06}Sb_{13.85}Bi_{26.05})_{91.83}(S_{113.79}Te_{0.11}Se_{0.2})_{114.1}$, respectively. The data form two clusters in Cu+Fe(+Ag)-Bi+Sb(+As)-Pb(+Cd) compositional space (Fig. 1c), with a slightly larger spread for izoklakeite than kobellite. The two sulfosalts form nanoscale intergrowths, as documented by imaging and variation in Pb and Bi distributions on EDS-STEM maps (Fig. 1d; Fig. A2, Appendix[1]).

According to Zakrzewski and Makovicky (1986), definition of homologues in the kobellite series considers two structural motifs: (i) larger $M_{6(N+1)}S_{7N+9}$ units based on the PbS archetype; and (ii) smaller PbS units with the general formula $M_{4N}S_{4(N+1)}$ based on a SnS-like structure. These motifs form a pseudotrigonal network of rods in both *a* and *b* directions and are interspersed with tetrahedrally coordinated (Cu, Fe) atoms for each pair of rods (Fig. 1a, b). Lead and Bi occur preferentially in the PbS-like motifs whereas Sb is concentrated in the SnS-like motifs. Incorporation of Ag is considered either

as substitution in the PbS rods, via Ag+Bi=2Pb, or filling interstitial vacancies (e.g., Cu+Pb=vacancy+Bi).

The main structural motifs and their arrangement are readily observed on HAADF STEM images with specimen tilted down to [001] zone axis (Fig. 2). The shorter SnS slab (slab 2) is darker than the larger PbS one (slab 1) in both cases, whereas each contact between two types of rods is marked by a still darker ribbon formed by intermittent 'spot'-like areas, only a few Å in width. The latter consist of the least bright, smallest atoms surrounded by 5 atoms of brightness comparable with those in the main two slabs (circled on Fig. 2a, b, upper right), suggesting these positions are occupied by Cu and Fe. Relative changes in grey shade across the array of the two main building slabs are concordant with the distribution of (Bi, Pb) and (Sb, Pb) in the PbS and SnS motifs, respectively. The two main slabs are twinned along the 34 Å-repeat ($b_{\text{kobellite}}$ and $a_{\text{izoklakeite}}$) and form stacks of thinner and thicker blocks parallel with one another, i.e., slab 1 + slab 2 at ~22.5 Å along $a_{\text{kobellite}}$, and ~38 Å along $b_{\text{izoklakeite}}$, on [001] in each sulfosalt. The homologue number for each species can be calculated directly from the sum of atoms in these two slabs using the formulae $N=n_1/6-1$ and $N=n_2/4$, where n_1 and n_2 are the number of atoms in the PbS and SnS slabs, respectively. Direct counting of n_1 and n_2 on the images gives $n_1=30$ and $n_2=16$ for izoklakeite, and $n_1=18$ and $n_2=8$ for kobellite (Fig. 2a, b, lower right). Considering the difficulty in calculating N for species with compositional variation in terms of Cu, Fe, and Ag substitution (Zakrzewski and Makovicky 1986), HAADF STEM imaging is a straightforward method to confirm homologue identity.

STEM modelling for izoklakeite shows a better fit between the images (Fig. 3) and the refined structural model for Bi-rich izoklakeite given by Makovicky and Mumme (1986) compared to that of Armbruster and Hummel (1987). This is despite the composition of the species considered here being very close to that in the second model (Sb/(Sb+Bi) = 0.35 and 0.395, respectively). One difference between the two crystal structural models is the occupancy of mixed (Sb, Bi, Pb) sites throughout the two main structural motifs. The present data shows that slab 1 and 2 are distinctly brighter and darker,

142 respectively, suggesting overall distributions of Sb and Bi within one or the other main slabs, i.e., Sb and
143 Bi preferring the SnS and PbS configurations. The model of Armbruster and Hummel (1987) should be
144 further proven by investigating mixed site occupancy, e.g., by atom-scale STEM-EDX mapping. STEM
145 simulations for kobellite using the crystal structure of Miehe (1971) shows the main structural motifs but
146 does not match the imaged atoms (Fig. A3, Appendix[1]), or the crystal structure model (Fig. 1a).
147 Selected-area of electron diffraction patterns taken down the [001] zone axis and Fast Fourier
148 Transforms obtained from images for izoklakeite and kobellite in this study show odd reflections of the
149 type $h00 \neq 2n$ and $0k0 \neq 2n$ which are incompatible with symmetry in *Pnnm* space group (Fig. A4,
150 Appendix[1]). Odd reflections along twin directions have been discussed with respect to differences in
151 twin/block thickness for Pb-Bi-sulfosalts (Colaïtis et al., 1981). The same effects likely cause non-
152 extinction Bragg reflections on both directions with slabs of different widths for the two chessboard
153 structures discussed here.
154 HAADF STEM imaging also reveals syntactic unit-cell-scale intergrowths between the two species
155 on [001] zone axis with $a_{\text{kobellite}} \,||\, b_{\text{izoklakeite}}$ (Fig. 4a, b). The intergrowths extend down to the scale of 1/2
156 unit cells on $b_{\text{izoklakeite}}$ and one unit on $a_{\text{kobellite}}$. Such crystal-structural modularity among homologues of
157 the same series, or between related structures, can account for rhythmic compositional banding down to
158 the nanoscale as has been documented for other Bi-Pb-sulfosalts and interpreted as primary growth
159 textures (e.g., Pring et al. 1999; Ciobanu et al. 2004; Pring and Ciobanu 2008). Secondary replacement
160 of izoklakeite is also observed as irregular slabs of kobellite 'intruding' into izoklakeite in associations
161 which display step-wise contacts between the two species (Fig. 4c). Both types of intergrowths, banded
162 and irregular, account for the compositional fields measured at the micron-scale (Fig. 1c).
163 Nanoscale intergrowths among members of Pb-Bi-sulfosalts from the same series or across series
164 sharing crystal-structural blocks have been predicted (e.g., Makovicky 1997), or documented elsewhere.
165 The presence of smallest atomic-scale intergrowths among different species of sulfosalts with chessboard

166 structures, is documented here for the two kobellite homologues and elsewhere for different Cu-bearing
167 neyite species (Ciobanu et al. 2016) and may be an inherent feature of their 2-D modular architectures.
168 Although the N=3 homologue of the kobellite series is also predicted (Makovicky and Mumme 1986),
169 this is not observed to occur here, the relevant compositional field being represented by intergrowths of
170 N=2 and N=4 phases.

171 ## IMPLICATIONS

172 Imaging in HAADF STEM mode is better suited than conventional BF TEM mode since it can directly
173 visualise heavy atoms forming motifs underpinning crystal-structural modularity in Pb-Bi-sulfosalts, as
174 well as stacking sequences in mixed layer compounds, e.g., REE-fluorocarbonates of the bastnäsite-
175 synchysite group, or Bi-tellurides from the tetradymite group (Ciobanu et al., 2017; Cook et al. 2017).
176 Crystal-structural modularity is a topic of considerable interest for the definition of equilibrium
177 conditions in natural systems or high-tech applications of 'smart' materials capable of accommodating
178 incremental compositional variation through nanoscale intergrowths (e.g., Dittrich et al. 2009).

179 **Acknowledgements**

180 We acknowledge the support the Australian Microscopy and Microanalysis Research Facility for instrument
181 access. Financial support for Wei Li was provided by the National "973" Program of China (2014CB440902), the
182 National Science Foundation of China (41573042 and 41372090) and the MNR Key Laboratory of Metallogeny
183 and Mineral Assessment, Institute of Mineral Resources, Chinese Academy of Geological Sciences (ZS1702).
184 Comments from Yves Moëlo and two anonymous reviewers are gratefully appreciated and allowed us to clarify
185 aspects of this manuscript.

186 ## REFERENCES CITED

187 Armbruster, T., and Hummel, W. (1987) (Sb,Bi,Pb) ordering in sulfosalts: crystal-structure refinement of a Bi-
188 rich izoklakeite. American Mineralogist, 72, 821–831.

189 Biagioni, C., and Moëlo, Y (2017) Lead-antimony sulfosalts from Tuscany (Italy). XIX. Crystal chemistry of

chovanite from two new occurrences in the Apuan Alps and its 8 Å crystal structure. Mineralogical Magazine, 81, 811–831.

Ciobanu, C.L., and Cook, N.J. (2000) Intergrowths of bismuth sulphosalts from the Ocna de Fier Fe-skarn deposit, Banat, Southwest Romania. European Journal of Mineralogy, 12, 899-917.

Ciobanu, C.L., Pring, A., and Cook, N.J. (2004) Micron- to nano-scale intergrowths among members of the cuprobismutite series and paděraite: HRTEM and microanalytical evidence. Mineralogical Magazine, 68, 279-300.

Ciobanu, C.L., Cook, N.J., Maunders, C., Wade, B.P., and Ehrig, K. (2016) Focused ion beam and advanced electron microscopy for minerals: insights and outlook from bismuth sulphosalts. Minerals, 6(4), 112; doi:10.3390/min6040112

Ciobanu, C.L., Kontonikas-Charos, A., Slattery, A., Cook, N.J., Ehrig, K., and Wade, B.P. (2017) Short-range stacking disorder in the bastnäsite-parisite compositional range: A HAADF-STEM study. Minerals, 7, 227; doi:10.3390/min7110227.

Colaïtis, D., van Dyck, D., and Amelinckx, S., (1981) Electron microscopic study of the system mPbS-$n$$Bi_2S_3$. Phys. Stat. sol. (a) 68, 419-438.

Cook, N.J., Ciobanu, C.L., Ehrig, K., Slattery, A., Verdugo-Ihl, M.R., Courtney-Davies, L., and Gao, W. (2017) Advances and opportunities in ore mineralogy. Minerals, 7(12), 233; doi:10.3390/min7120233.

Dittrich, H., Stadler, A., Topa, D., Schimper, H.-J., and Basch, A. (2009) Progress in sulfosalt research. Physica Status Solidi (A) Applications and Materials Science 206, 1034-1041.

Donovan, J.J., Singer, J.W., and Armstrong, J.T., 2016. A new EPMA method for fast trace element analysis in simple matrices. American Mineralogist, 101, 1839–1853.

Doussier, C., Moëlo, Y., Meerschaut, A., Léone, P., and Guillot-Deudon, C. (2008) Crystal structure of the new compound $Pb_{3+x}Sb_{3-x}S_{7-x}Cl_{1+x}$(x~0.45): The homologous series $Pb_{(2+2N)}(Sb,Pb)_{(2+2N)}S_{(2+2N)}(S,Cl)_{(4+2N)}Cl_N$ and its polychalcogenide derivatives (N = 1–3). Journal of Solid State Chemistry, 181, 920–934.

Graeser, S. (1963) Giessenit — ein neues Pb–Bi–Sulfosalz aus dem Dolomit des Binnatals. Schweiz. Mineralogisches Petrographisches Mitteilungen, 43, 471–478.

Graeser, S., and Harris, D.C. (1986) Giessenite from Giessen near Binn, Switzerland: new data. Canadian

Mineralogist, 24, 19–20.

Harris, D.C., Jambor, J.L., Lachance, G.R., and Thorpe, R.I. (1968) Tintinaite, the antimony analogue of kobellite. Canadian Mineralogist, 9, 371–382.

Harris, D.C., Roberts, A.C., and Criddle, A.J. (1986) Izoklakeite, a new mineral species from Izok Lake, Northwest Territories. Canadian Mineralogist, 24, 1–5.

Kryukova, G.N., Heuer, M., Wagner, G., Doering, T., and Bente, K. (2005) Synthetic $Cu_{0.507(5)}Pb_{8.73(9)}Sb_{8.15(8)}I_{1.6}S_{20.0(2)}$ nanowires. Journal of Solid State Chemistry, 178, 376-381.

Li, W., Cook, N.J., Xie, G.Q., Mao, J.W., and Ciobanu, C.L. (2019a) Trace element distributions in (Cu)-Pb-Sb sulfosalts from the Gutaishan Au-Sb deposit, South China: Implications for formation of high-fineness gold. American Mineralogist.

Li, W., Cook, N.J., Xie, G.Q., Mao, J.W., Ciobanu, C.L., Li, J.W., and Zhang, Z.Y. (2019b) Textures and trace element signatures in pyrite and arsenopyrite from the Gutaishan Au-Sb deposit, South China. Mineralium Deposita. https://doi.org/10.1007/s00126-018-0826-0

Makovicky, E. (1997) Modular aspects of sulfides and sulfosalts. In: EMU Notes in Mineralogy: Modular Aspects of Minerals (S. Merlino, Ed.), European Mineralogical Union, Jena, Germany, Volume 1, p. 237–271.

Makovicky, E., and Karup-Møller, S. (1986) New data on giessenite from the Bjørkåsen sulfide deposit at Otoften, northern Norway. Canadian Mineralogist, 24, 21–25.

Makovicky, E., and Mumme, W.G. (1986) The crystal structure of izoklakeite, $Pb_{51.3}Sb_{20.4}Bi_{19.5}Ag_{1.2}Cu_{2.9}Fe_{0.7}S_{114}$. The kobellite homologous series and its derivatives. Neues Jahrbuch für Mineralogie Abhandlungen, 153, 121–145.

Miehe, G. (1971) The crystal structure of kobellite. Nature, Physical Science, 231, 133–134.

Moëlo, Y., Jambor, J.L., and Harris, D.C. (1984) Tintinaïte et sulfosels associés de Tintina (Yukon): la cristallochimie de la série de la kobellite. The Canadian Mineralogist, 22, 219–226.

Moëlo, Y., Roger, G., Maurel-Palacin, D., Marcoux, E., and Loroussi, A. (1995) Chemistry of some Pb-(Cu,Fe)-(Sb,Bi) sulfosalts from France and Portugal. Implications for the crystal chemistry of lead sulfosalts in the Cu-poor part of the Pb_2S_2–Cu_2–Sb_2S_3–Bi_2S_3 system. Mineralogy and Petrology, 53, 229–250.

Moëlo, Y., Makovicky, E., Mozgova, N.N., Jambor, J.L., Cook, N.J., Pring, A., Paar, W., Nickel, E.H., Graeser,

G., Karup-Møller, S., Balic-Žunic, T., Mumme, W.G., Vurro, F., Topa, D., Bindi, L., Bente, K., and Shimizu, M. (2008) Sulfosalt systematics: A review. Report of the Sulfosalt Sub-Committee of the IMA Commission on Ore Mineralogy. European Journal of Mineralogy, 20, 7–46.

Ozawa, T., Saitow, A., and Hori, H. (1998) Chemistry and crystallography of Bi-rich izoklakeite from the Otome mine, Yamanashi Prefecture, Japan and discussion of the izoklakeite-giessenite series. Mineralogical Journal, 20, 179-187.

Pring, A., and Ciobanu, C.L., 2008. Chemical modulations in Pb-Bi-sulphosalts: a glimpse at minerals in solid-state chemistry. In: Harris, K., Edwards, P. (Eds.), Turning Points in Solid State, Materials and Surface Chemistry. Royal Society of Chemistry Publishing, p. 239-249.

Pring, A., Jercher, M., and Makovicky, E. (1999) Disorder and compositional variation in the lillianite homologous series. Mineralogical Magazine, 63, 917–926.

Utsunomiya, S., Palenik, C.S., Valley, J.W., Cavosie, A.J., Wilde, S.A., and Ewing, R.C. (2004) Nanoscale occurrence of Pb in an Archean zircon. Geochimica et Cosmochimica Acta, 68, 4679–4686.

Xu, H., Shen, Z., and Konishi, H. (2014) Si-magnetite nano-precipitates in silician magnetite from banded iron formation: Z-contrast imaging and ab initio study. American Mineralogist, 99, 2196–2202.

Zakrzewski, M.A., and Makovicky, E. (1986) Izoklakeite from Vena, Sweden, and the kobellite homologous series. The Canadian Mineralogist, 24, 7–18.

Figure captions

Figure 1. Atom filling models of kobellite (a) and izoklakeite (b) on [001] zone axis obtained using data from Miehe (1971) and Armbruster and Hummel (1987), respectively. Unit cells (Å) for kobellite: a=22.575; b=34.104; c=4.038; and izoklakeite: a=34.221; b=37.933; c=4.063; space groups for both are *Pnnm*. (c) Cu+Ag(+Fe)-Bi+Sb-Pb+(Cd) ternary diagram showing composition of the two sulfosalts. Grey stars represent ideal Pb-Bi-sulfosalts added for reference. (d) EDS-STEM map of nanoscale intergrowths between the two analysed sulfosalts.

Figure 2. HAADF STEM images showing kobellite (a) and izoklakeite (b) on [001] zone axis. The PbS (brighter) and SnS (darker) motifs are stacked alternatively along the b axis whereas 'twinning' of PbS and SnS motifs is apparent along a. Bright dots represent heavy atoms with size decreasing in the order Bi, Pb (white circles), to Sb

(yellow circles) as highlighted in images bottom-right. Mixed sites may be present but cannot be resolved. Smallest atoms (Cu, Fe), located at the junction between the two main motifs, are highlighted in images top-right. The images (bottom right) allow calculation of the homologue number as N=n1/6-1 and N=n2/4, where n1 and n2 are the number of atoms in the PbS and SnS motifs, respectively.

Figure 3. STEM simulations of izoklakeite on [001] zone axis using crystal structures from Makovicky and Mumme (1986) in (a), and Armbruster and Hummel (1987) in (b). Unit cell in yellow, PbS and SnS motifs highlighted as blue and yellow shades. HAADF STEM image (c) shows a better fit with (a), i.e., the contrast between the two atoms within the modules, and between the two modules, does not vary much due to mixed sites as in (b).

Figure 4. HAADF STEM images showing rhythmic banding between kobellite and izoklakeite (a, b) and replacing relationships in (c). The smallest repeats between PbS (green in izoklakeite and blue in kobellite) and SnS (yellow in izoklakeite and orange in kobellite) stacks along the $b_{\text{izokalkeite}}$ *and* $a_{\text{kobellite}}$ are shown in (b).

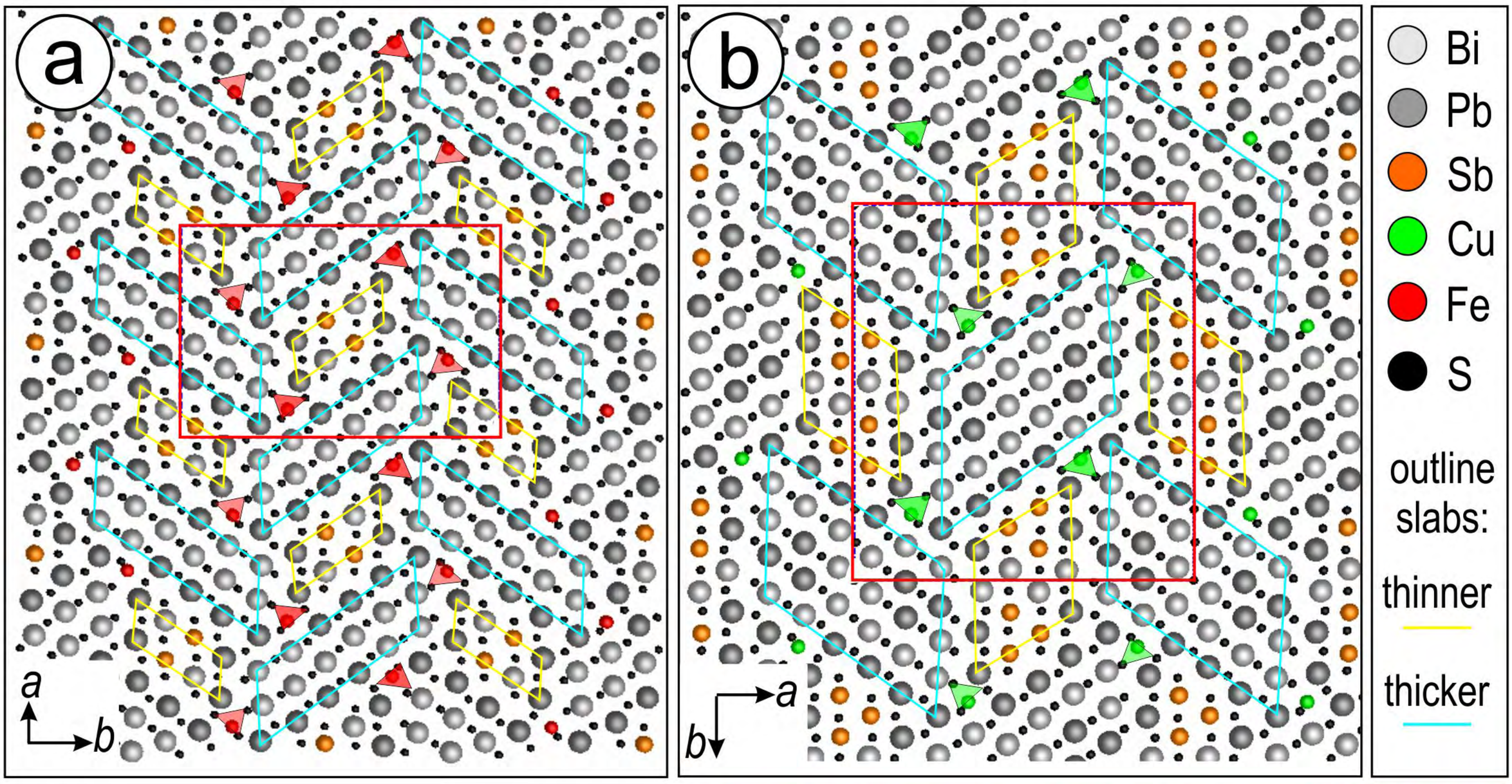

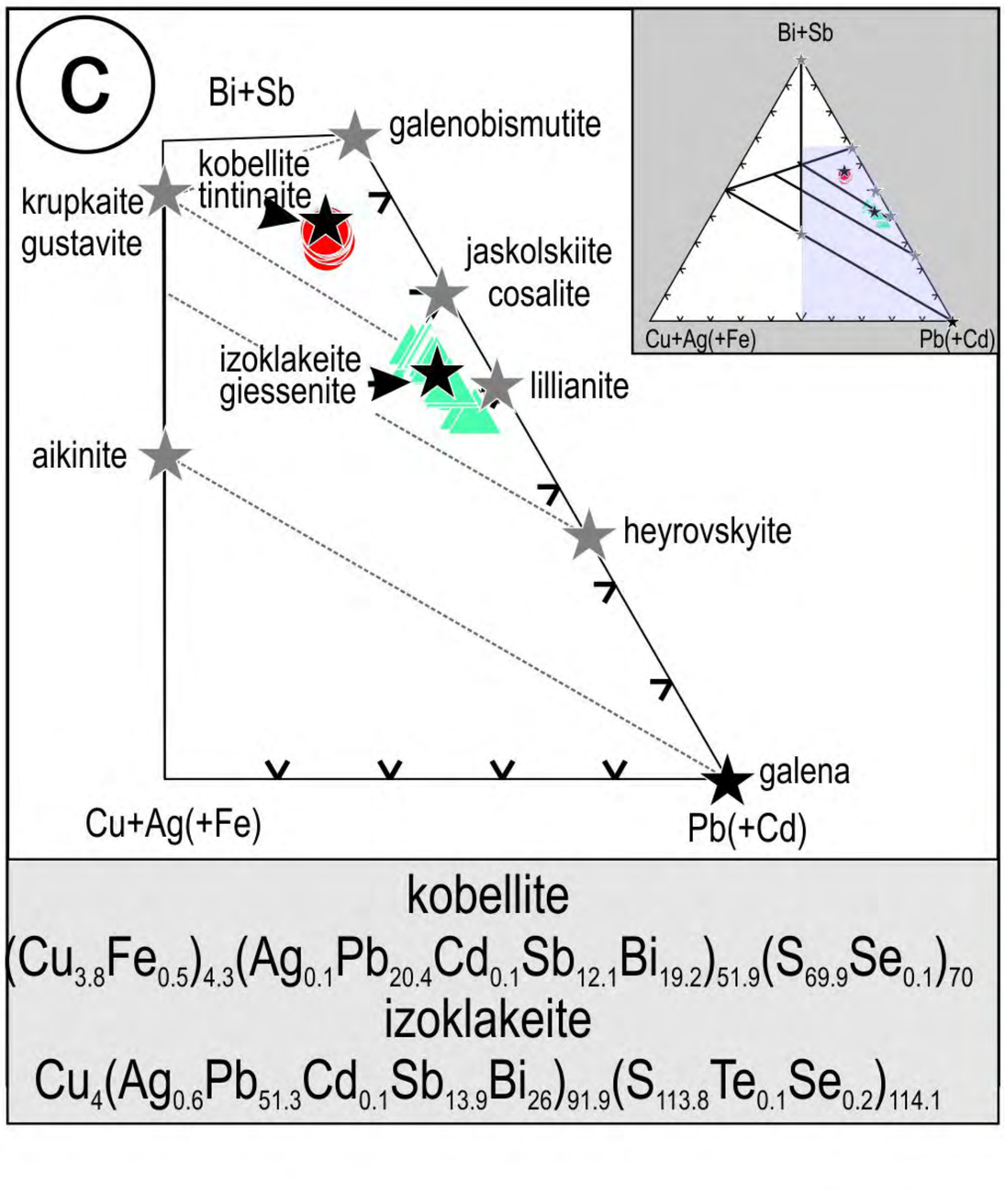

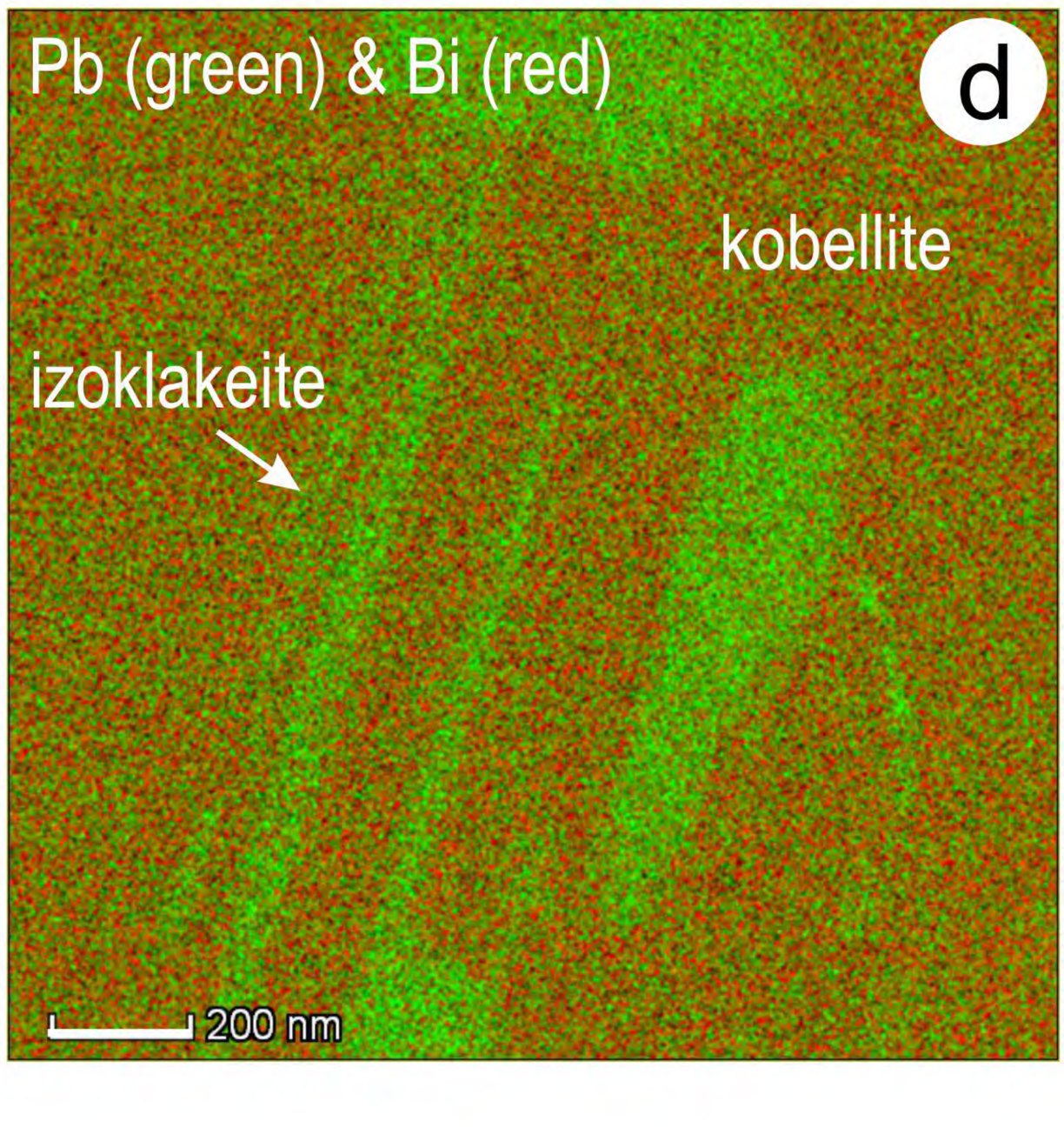

Li et al., Figure 1

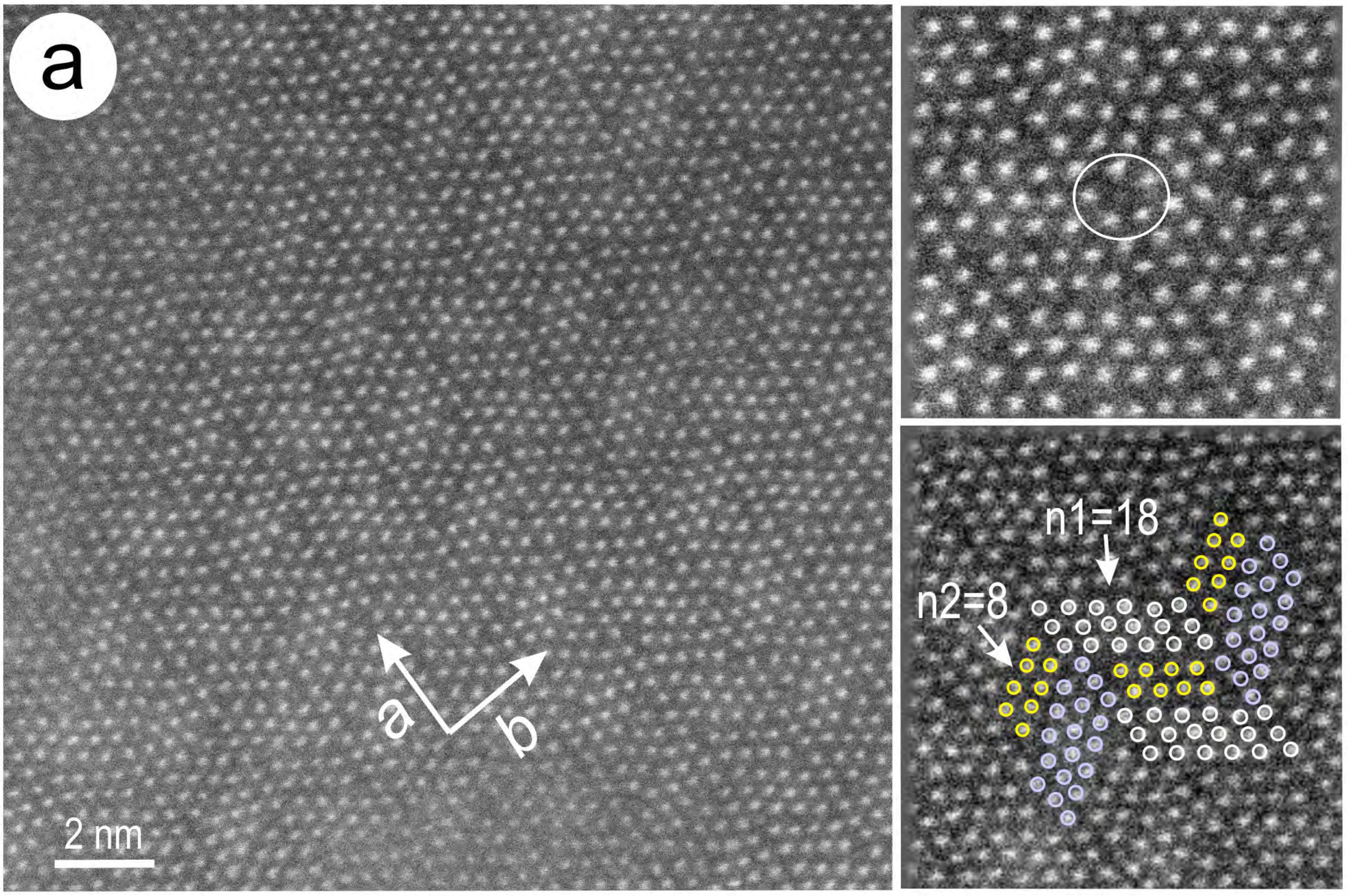

Li et al., Figure 2

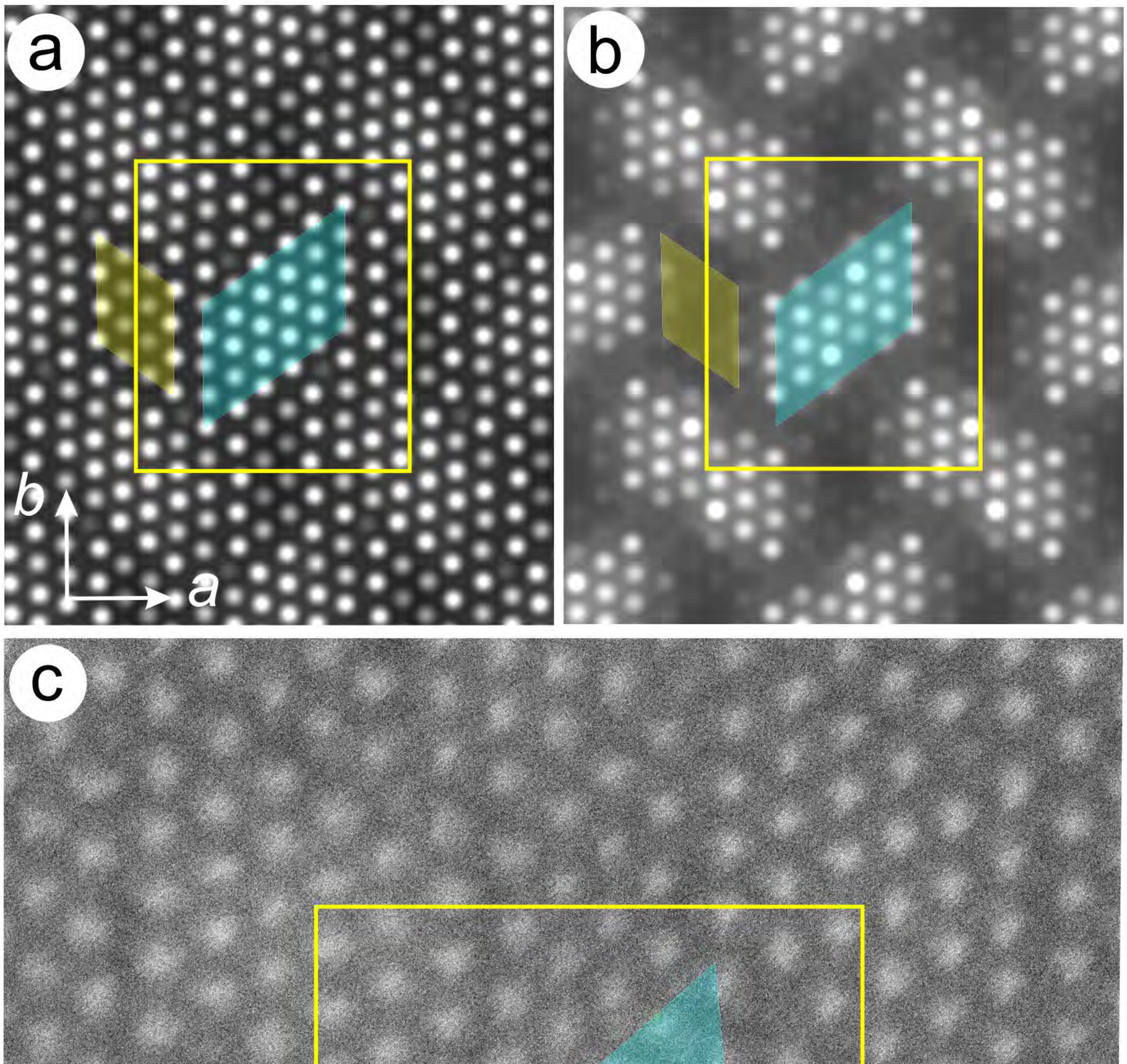

Li et al., Figure 3

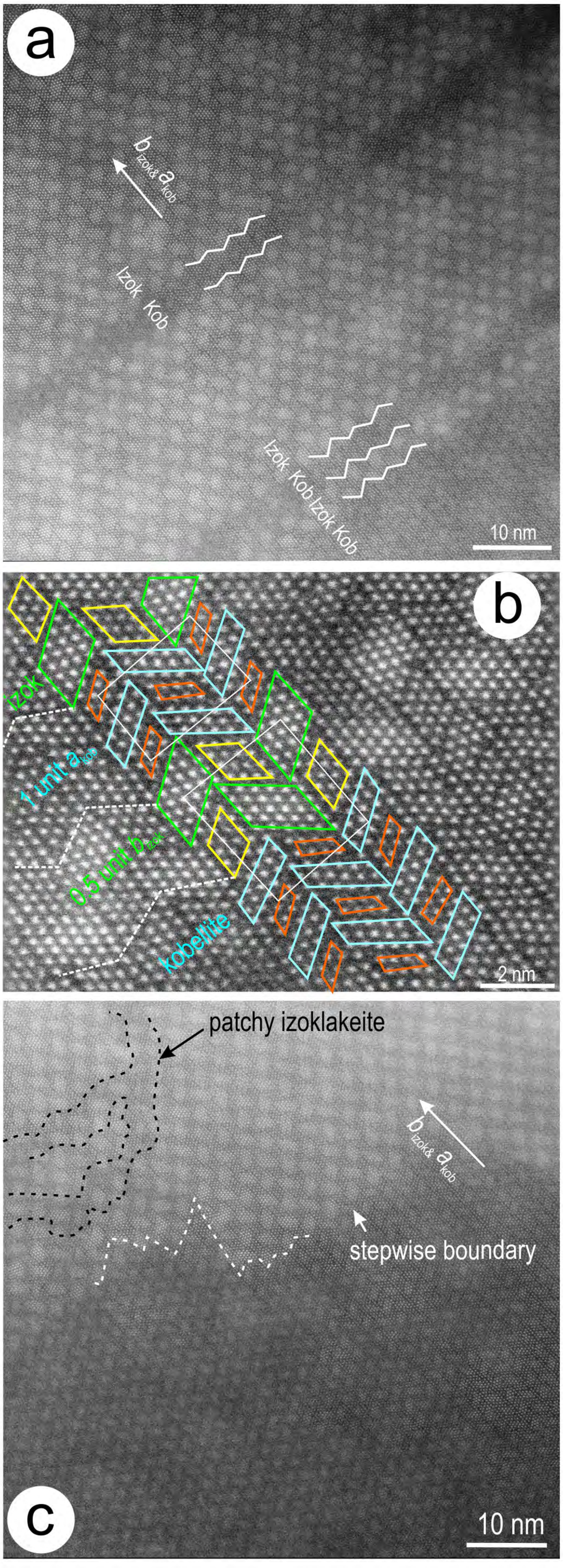

Li et al., Figure 4